



## Dynamic Stability Enhancement in Low-Inertia Power Systems Using Battery Energy Storage

Jannesar, Mohammad Rasol; Sadr, Sajad; Savaghebi, Mehdi

*Published in:*  
Proceedings of 2022 12th Smart Grid Conference (SGC)

*Link to article, DOI:*  
[10.1109/SGC58052.2022.9998974](https://doi.org/10.1109/SGC58052.2022.9998974)

*Publication date:*  
2023

*Document Version*  
Peer reviewed version

[Link back to DTU Orbit](#)

*Citation (APA):*  
Jannesar, M. R., Sadr, S., & Savaghebi, M. (2023). Dynamic Stability Enhancement in Low-Inertia Power Systems Using Battery Energy Storage. In *Proceedings of 2022 12th Smart Grid Conference (SGC) IEEE*. <https://doi.org/10.1109/SGC58052.2022.9998974>

---

### General rights

Copyright and moral rights for the publications made accessible in the public portal are retained by the authors and/or other copyright owners and it is a condition of accessing publications that users recognise and abide by the legal requirements associated with these rights.

- Users may download and print one copy of any publication from the public portal for the purpose of private study or research.
- You may not further distribute the material or use it for any profit-making activity or commercial gain
- You may freely distribute the URL identifying the publication in the public portal

If you believe that this document breaches copyright please contact us providing details, and we will remove access to the work immediately and investigate your claim.

# Dynamic Stability Enhancement in Low-Inertia Power Systems Using Battery Energy Storage

Mohammad Rasol Jannesar  
 Department of Electrical Engineering  
 Technical and Vocational University  
 (TVU)  
 Tehran, Iran  
[mjannesar@tvu.ac.ir](mailto:mjannesar@tvu.ac.ir)

Sajad Sadr  
 Department of Electrical Engineering  
 Tafresh University  
 Tafresh, Iran  
[sadr@tafreshu.ac.ir](mailto:sadr@tafreshu.ac.ir)

Mehdi Savaghebi  
 Department of Engineering Technology  
 Technical University of Denmark  
 DK-2750 Ballerup, Demark  
[medi@dtu.dk](mailto:medi@dtu.dk)

**Abstract**—By increasing the number of inverter-based resources, for instance wind turbines (WTs), the overall inertia of the network and the dynamic frequency and voltage stability are decreased. Proper battery energy storage system (BESS) control can improve stability in this case. In this paper, by considering a low-inertia power grid facing loss of generation, the effect of BESS on stability enhancement is evaluated. The study network is a modified Kundur’s four-machine system modeled in PowerFactory. The results show that BESS can reduce fluctuations and increase the stability of the system.

**Keywords**— voltage and frequency stability, BESS, wind turbine, low-inertia grid and transmission system.

## I. INTRODUCTION

Nowadays, due to environmental problems, the use of renewable energy resources (RESs) has been developed. Different references like [1-4] have dealt with the growing interest in utilization of RESs. For instance, the trend of RESs development in the last decade is illustrated in Fig. 1 [1]. Due to the fact that RESs such as wind turbines (WTs) and photovoltaics (PVs), unlike traditional power plants, are connected to the network by power electronic, the inertia of the network is reduced as a result of high penetration of renewables [5]. Some aspect of impact of RESs versus traditional synchronous generator (SG) on power system stability are considered in [6, 7]. Substituting SGs by RESs creates different issues in the power system, e.g., flexibility and stability problems as discussed in [8] and [9], respectively.

When there is a fault or change in the load and generation of the network, the reduction of inertia can make the network more fluctuating or even unstable [10]. During disturbances,

one of the solutions is the use of battery energy storage system (BESS), which with proper control can increase network stability by injecting active and reactive power [11].

In [12], a frequency responsive BESS model is proposed to improve the frequency response of a low-inertia power system. In [13], the effect of ESS location on primary frequency support is presented in networks with significant penetration of RESs. The extensive investigations are carried out in [14] to explore the roles of superconducting magnetic energy storage and BESS for improving the frequency response of a low-inertia grid. To avoid under frequency load shedding, BESSs are being installed in [15] and injected active power at generation loss. The application of BESSs is investigated in [16] for primary frequency control in power systems with very high penetration of renewable energy. A control model for frequency stabilization was developed in [17] for low-inertia power systems. In [18], it is indicated that BESS’s controller has significant impact on the damping of electromechanical oscillation mode. The authors in [19] perform an in-depth analysis of BESS impact in providing primary frequency control to support increased WT penetration. In these papers voltage stability is not considered.

In the present paper, the stability of both frequency and voltage is improved by considering a suitable control method for the BESS in a low-inertia grid.

The rest of the paper is organized as follows. Section II describes the BESS modeling and control. Section III contains simulation results and relevant analyses. Finally, Section IV outlines the main findings to conclude the paper.

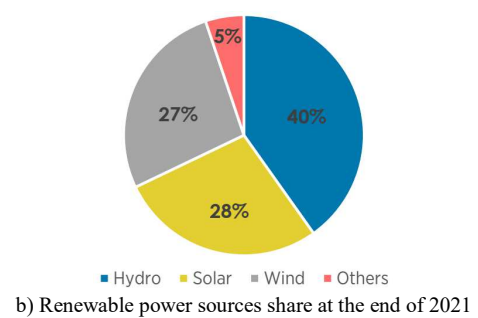
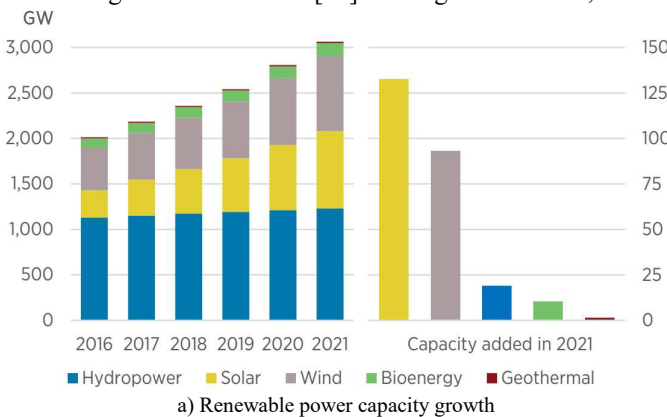


Fig. 1. Worldwide renewable power generation installed capacity (GW) [1]

## II. BESS MODELING AND CONTROL

In this paper, a fully-rated converter (FRC) WT model is used, which is more common in new designs, especially in high power. The block diagram (Fig. 2) has been used to model WT [20].

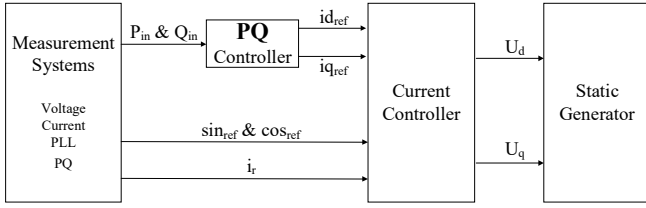


Fig. 2. WT model [20]

As it can be seen, at first, the voltage, current and active and reactive powers are measured from the point of common coupling (PCC) of the WT, and  $\sin_{ref}$  and  $\cos_{ref}$  are calculated by the phase-locked loop (PLL). The measured active and reactive power values ( $P_{in}$  and  $Q_{in}$ ) are entered into the PQ Control block and create reference dq-current ( $i_{dref}$  and  $i_{qref}$ ). These dq-current along with  $\sin_{ref}$ ,  $\cos_{ref}$  and the real current component ( $i_r$ ) by entering the current controller block produce dq-voltage ( $u_d$  and  $u_q$ ) which are the input of the WT generator block diagram.

In BESS controller, d-axis and q-axis are two current parameters that should be controlled. The d-axis and q-axis components control active and reactive power, respectively. With the active and reactive power, the frequency and voltage could be controlled, respectively. In Fig. 3, the block diagram for BESS controller is introduced.

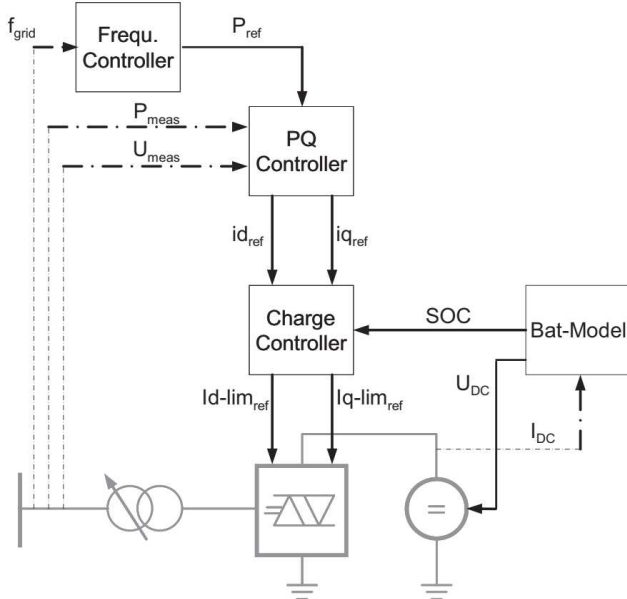


Fig. 3. BESS controller [21]

As can be seen, the frequency, power and voltage of the network are measured. The frequency of the network is entered into the frequency controller block and makes the reference power. The reference power along with the measured power and voltage is entered into the PQ controller block and produces the reference current of the dq-frame. These currents produce reference limited dq-currents according to the state of charge (SOC) in the charge controller block, which are given to the inverter.

In Fig. 4, the block diagram for BESS modeling is expanded [22]. The description and value for variables of Fig. 4 are provided in Table I.

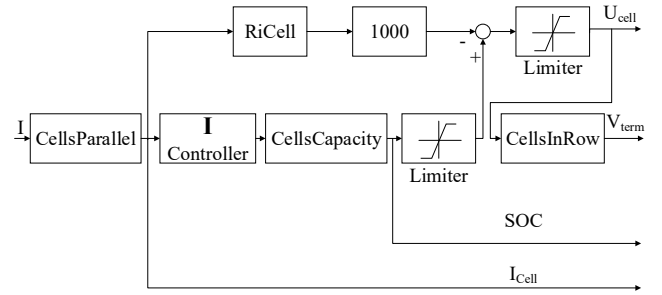


Fig. 4. BESS model

TABLE I. PARAMETERS OF BESS MODEL

Variable	Description	Parameter	Unit
SOC0	State of charge at initialisation	80	%
CellsCapacity	Capacity per cell	80	Ah
CellsParallel	Number of parallel cells	60	-
CellsInRow	Number of cells in row	65	-
RiCell	Intern Resistance per cell	0.001	ohm

The SOC is calculated with an integrator, counting the current of the battery

$$U_{DC} = U_{max} \cdot SOC + U_{min} \cdot (1 - SOC) - I \cdot Z_i \quad (1)$$

where  $U_{min}$  and  $U_{max}$  are voltage of discharged and fully-charged cell, respectively. Also,  $I$  is the discharge current and  $Z_i$  is inner resistance.

The whole controller (Fig. 3) can be divided in smaller parts such as PQ, frequency, and charge controller shown in Figs. 5, 6 and 7.

In Fig. 5 the block diagram for PQ controller is described [22].

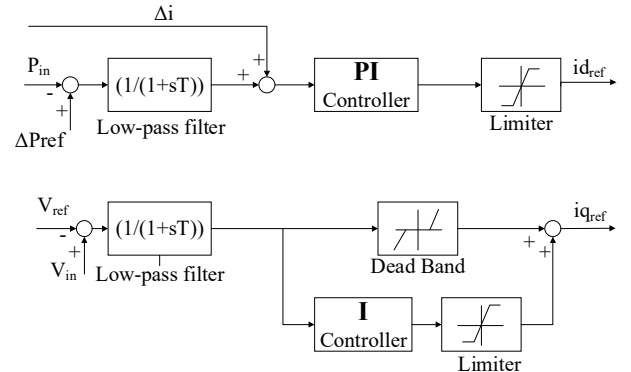


Fig. 5. PQ controller

As can be seen, the difference between the input power and the reference power is given to the low-pass filter and then adding with  $\Delta i$  that is the difference between  $I_{dref}$  and  $I_{dref(out)}$

(see Fig. 7). This signal is given to the PI controller and after passing through the limiter makes the  $I_{dref}$ . On the other hand, the difference between the input and the reference voltage (respectively  $V_{in}$  and  $V_{ref}$ ) after passing through the low-pass filter is fed to the I Controller and Dead Band blocks. The sum of these two signals makes the  $I_{qref}$ .

In Fig. 6, the block diagram for frequency controller is indicated [22].

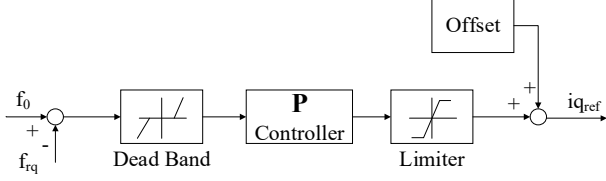


Fig. 6. Frequency controller

As can be seen, the frequency difference is given to the Dead Band and after passing through the P controller and the limiter, it is added with the offset value and makes the  $I_{qref}$ .

In Fig. 7, the block diagram for charge controller is shown [22].

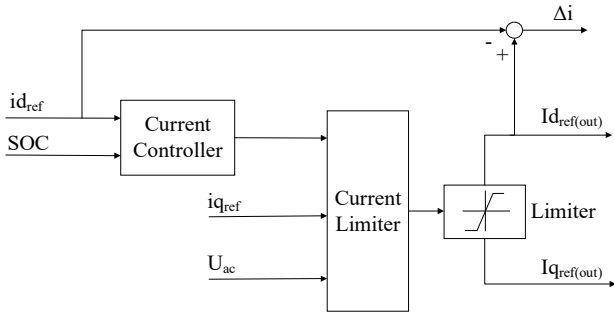


Fig. 7. Charge controller

As it can be seen,  $I_{dref}$  and SOC are entered into the current controller, and the output of this controller along with the  $I_{dref}$  and  $U_{ac}$  are entered into the current limiter block. The output of this block, after passing through the limiter, makes the  $I_{dref}$  (out) and  $I_{qref}$  (out).

### III. SIMULATION RESULTS

The study network is a modified Kundur's four-machine system modeled in PowerFactory and can be seen in Fig. 8 [23].

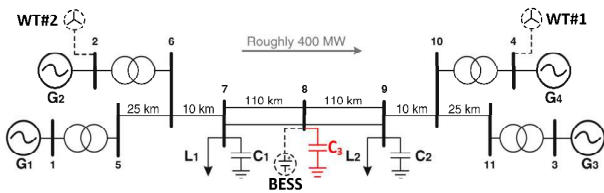


Fig. 8. Modified Kundur's four-machine system

In this system, the capacitor  $C_3$  with a capacity of 100 MVar is added to Bus 8 for increasing the bus voltage to a range suitable for the simulation study [22].

The size of SGs, WTs, BESS, loads, and capacitors is reported in Table II.

In order to investigate the effect of increasing the penetration of WTs and adding BESS on the frequency and

voltage stability, two scenarios have been considered: Case 1-Network with 1 WT and Case 2-Network with 2 WTs.

TABLE II. THE SIZE OF NETWORK EQUIPMENT

Bus	$P_G$ (MW)	$P_L$ (MW)	$Q_L$ (MVar)	$Q_C$ (MVar)
I(Slack)				
2	$G_2$ and WT#2 =700			
3	$G_3$ =719			
4	$G_4$ and WT#1 =700			
7		967	100	200
8	BESS=30			100
9		1767	100	350

In each of these scenarios, the network voltage and frequency are evaluated with and without BESS and WT. First, the voltage and frequency of the network without WT and BESS, then with WT and without BESS and finally with WT and BESS have been shown and analyzed.

#### A. Network with 1 WT

In this case, WT#1 is added and the synchronous machine  $G_4$  is replaced by this WT. Then the voltage and frequency stability of the network is evaluated versus 13% decrease in  $G_1$  production.

In Figs. 9 and 10, the frequency and voltage variations are illustrated, respectively. As can be seen, with the increase of WT penetration, the frequency of the network becomes unstable (violates the allowable range). By adding a 30 MW BESS to Bus 8, the network frequency becomes stable (within  $\pm 0.2$  Hz).

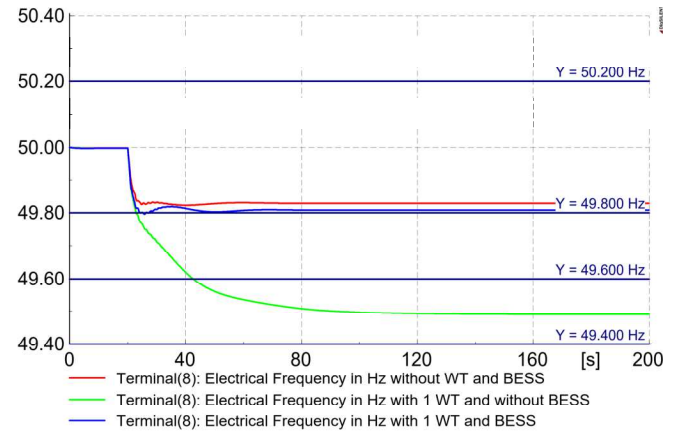


Fig. 9. Frequency stability in Case 1

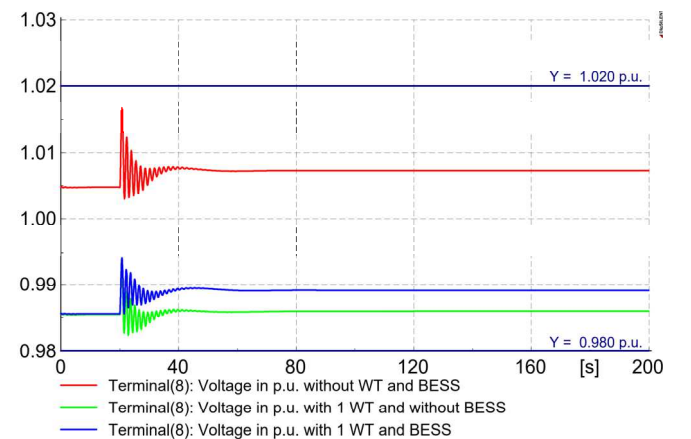


Fig. 10. Voltage stability in Case 1

In Fig. 11 the total active and reactive power of BESS is illustrated. According to the Fig. 11, when generation decreases as reflected by the frequency drop, the active power of the BESS increases to compensate lack of production.

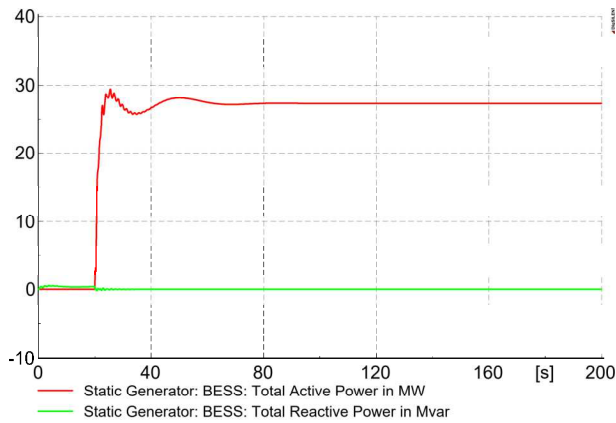


Fig. 11. Active and reactive power of BESS in Case 1

### B. Network with 2 WTs

In this scenario, WT#2 is also added to the network and the synchronous machine  $G_2$  is replaced by this WT so that a total of 2 WTs are added to the network. Similar to Case 1, the voltage and frequency stability of the network is evaluated against 13% decrease in  $G_1$  production.

In Figs. 12 and 13, the frequency and voltage stability are depicted, respectively.

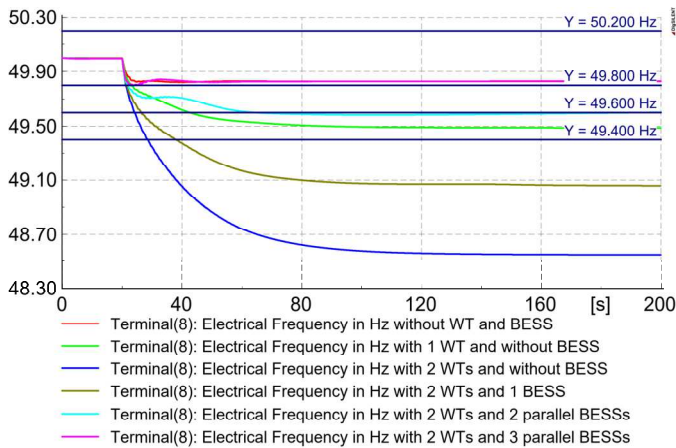


Fig. 12. Frequency stability in Case 2

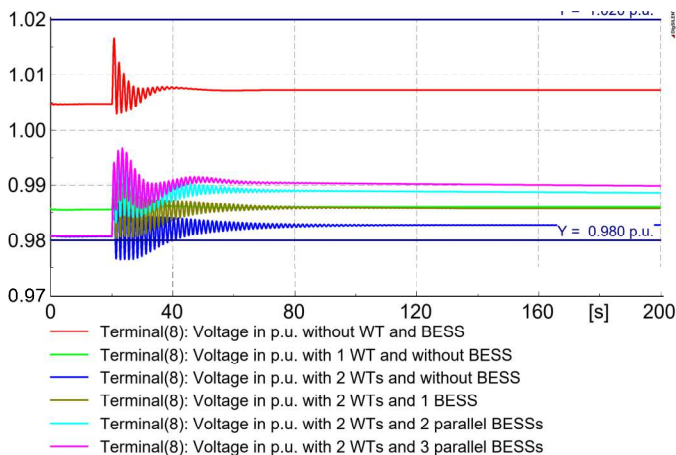


Fig. 13. Voltage stability in Case 2 conclusion

As can be seen, with the increase of WTs penetration (2 WTs), the network becomes unstable in terms of voltage (out of the  $\pm 2\%$ ) and frequency (out of the  $\pm 0.2$  Hz). To stabilize the network, by adding 1 and 2 parallel BESSs connected to Bus 8 (each with a capacity of 30 MW), the frequency does not return to the stable range. When 3 parallel BESSs are connected in this bus, the frequency and voltage become stable.

In Fig. 14 the total active and reactive power of BESS elucidated. As can be seen, the active power injected into the network is three times of that in the Case 1.

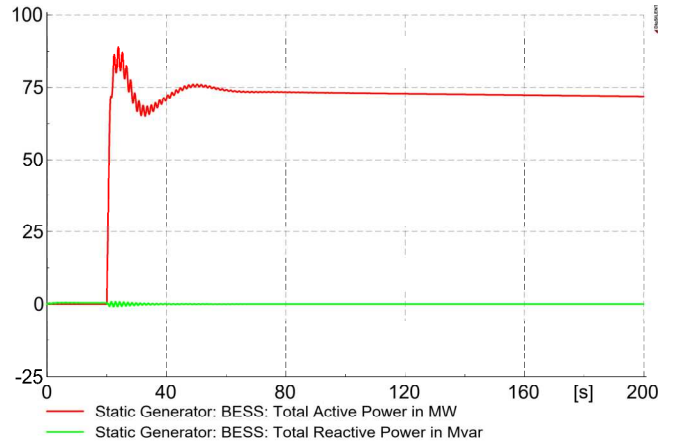


Fig. 14. Active and reactive power of BESS in Case 2

## IV. CONCLUSION

As it was observed, by increasing the penetration of WT, due to the decrease of grid inertia, the voltage and frequency stability of the network is affected. With addition of one WT, the network frequency became unstable which was stabilized by installing a BESS. Also, in order to stabilize the network with two WTs, three BESSs should be placed in parallel in Bus 8. At the moment of generation reduction, the BESS can stabilize the network frequency and voltage by injecting active and reactive power, respectively.

## REFERENCES

- [1] "<https://www.irena.org>." [Accessed: 11 September 2022].
- [2] B. K. Bose, *Power Electronics in Renewable Energy Systems and Smart Grid: Technology and Applications*. John Wiley & Sons, 2019.
- [3] B. Wu, Y. Lang, N. Zargari, and S. Kouro, *Power Conversion and Control of Wind Energy Systems*. John Wiley & Sons, 2011.
- [4] V. Yaramasu and B. Wu, *Model Predictive Control of Wind Energy Conversion Systems*. John Wiley & Sons, 2016.
- [5] D. A. kez *et al.*, "A critical evaluation of grid stability and codes, energy storage and smart loads in power systems with wind generation," *Energy*, vol. 205, 2020, doi: 10.1016/j.energy.2020.117671.
- [6] A. Fernández-Guillamón, E. Gómez-Lázaro, E. Muljadi, and Á. Molina-García, "Power systems with high renewable energy sources: A review of inertia and frequency control strategies over time," *Renewable and Sustainable Energy Reviews*, vol. 115, pp. 1-12, 2019.
- [7] H. Golpîra, A. Román-Messina, and H. Bevrani, *Renewable Integrated Power System Stability and Control*. John Wiley & Sons, 2021.
- [8] S. Impram, S. V. Nese, and B. Oral, "Challenges of renewable energy penetration on power system flexibility: A survey," *Energy Strategy Reviews*, vol. 31, 2020.
- [9] L. Meegahapola and D. Flynn, "Impact on transient and frequency stability for a power system at very high wind penetration," presented at the IEEE PES General Meeting, 2010.
- [10] Y. Cheng, R. Azizpanah-Abarghoee, S. Azizi, L. Ding, and V. Terzija, "Smart frequency control in low inertia energy systems based on frequency response techniques: A review," *Applied Energy*, vol. 279, pp. 1-16, 2020.

- [11] C. Mosca *et al.*, "Mitigation of frequency stability issues in low inertia power systems using synchronous compensators and battery energy storage systems," *IET Gener. Transm. Distrib.*, vol. 13, no. 17, pp. 3951-3959, 2019.
- [12] M. N. H. Shazon, H. M. Ahmed, Z. Tasnim, M. A. Rahman, and Nahid-Al-Masood, "Frequency Response and Its Improvement Using BESS in a Low Inertia Power System," presented at the TENCON 2019 - 2019 IEEE Region 10 Conference (TENCON), 2019.
- [13] A. Adrees, J. V. Milanović, and P. Mancarella, "The Influence of Location of Distributed Energy Storage Systems on Primary Frequency Response of Low Inertia Power Systems," presented at the IEEE Power & Energy Society General Meeting (PESGM), 2018.
- [14] M. N. H. Shazon, Nahid-Al-Masood, H. M. Ahmed, S. R. Deeba, and E. Hossain, "Exploring the Utilization of Energy Storage Systems for Frequency Response Adequacy of a Low Inertia Power Grid," *IEEE Access*, vol. 9, pp. 129933-129950, 2021, doi: 10.1109/ACCESS.2021.3114216.
- [15] C. D. Aluthge, K. T. M. U. Hemapala, and J. R. Lucas, "Using BESS to Achieve Power System Dynamic Stability when High Solar Penetration is present: Case study Sri Lanka," presented at the 2nd International Conference on Smart Power & Internet Energy Systems (SPIES), 2020.
- [16] M. R. Amin, M. Negnevitsky, E. Franklin, K. S. Alam, and S. B. Naderi, "Application of Battery Energy Storage Systems for Primary Frequency Control in Power Systems with High Renewable Energy Penetration," *Energies* vol. 14, no. 5, 2021, doi: 10.3390/en14051379.
- [17] L. Toma *et al.*, "On the virtual inertia provision by BESS in low inertia power systems," presented at the IEEE International Energy Conference (ENERGYCON), 2018.
- [18] H. Setiadi, N. Mithulananthan, and M. J. Hossain, "Impact of battery energy storage systems on electromechanical oscillations in power systems," presented at the IEEE Power & Energy Society General Meeting, 2017.
- [19] U. Datta, A. Kalam, and J. Shi, "The relevance of large-scale battery energy storage (BES) application in providing primary frequency control with increased wind energy penetration," *Journal of Energy Storage*, vol. 23, pp. 9-18, 2019.
- [20] D. Gusain, "Parameter Identification of Dynamic Equivalents for Active Distribution Systems using Heuristic Optimisation Techniques," Master, Delft University of Technology, 2016.
- [21] "Battery Energy Storing Systems," DlgSILENT PowerFactory, 2010.
- [22] F. M. Gonzalez-Longatt and J. L. R. Torres, *Modelling and Simulation of Power Electronic Converter Dominated Power Systems in PowerFactory*. Springer, 2021.
- [23] R. Preece, *Improving the Stability of Meshed Power Networks*. Springer, 2013.